The following article appeared in Geosphere (2010) 6 (1): 35–46; and may be found at: https://doi.org/10.1130/GES00204.1

Magnetic characteristics of fracture zones and constraints on the subsurface structure of the Colima Volcanic Complex, western Mexico

Hector Lopez-Loera
Instituto Potosino de Investigación Científica y Tecnológica, Camino a la Presa San José 2055, Lomas 4ª Sección, 78216, San Luis Potosí, S.L.P., Mexico

Jaime Urrutia-Fucugauchi*
Luis M. Alva-Valdivia
Laboratorio de Paleomagnetismo y Geofísica Nuclear, Instituto de Geofísica, Universidad Nacional Autonoma de México, Coyoacán 04510 Mexico D.F., Mexico

ABSTRACT

Detailed magnetic anomaly surveys over the central and southern sector of the Colima rift, western Mexico, are used to investigate the subsurface structure and faults and/or fractures in the volcanic terrains formed by activity in the Colima volcanic complex (CVC). The CVC is located within the large north-south Colima rift in western Mexico. The Colima rift is a major active tectonic structure, trending perpendicular to the Middle America Trench and related to subduction of the Rivera and Cocos plates. Volcanic activity in the CVC has migrated southward toward the trench. Analyses of faults and recent deformation in the CVC and Colima rift are of major interest in volcano-tectonic studies and for hazard assessment. Structural analyses and fault mapping, however, are difficult because young volcanic and pyroclastic rocks obscure structural features and stratigraphy. Most of the southern Colima rift is covered by volcanic avalanches and volcaniclastic units, which have resulted in resurfacing of the volcanic terrains. Here we show that magnetic anomalies permit identification of faults and mapping of volcano-sedimentary and volcanic units. Total magnetic field measurements spaced every 0.5 km along 8 profiles, with an overall length of 284.5 km and covering the CVC sector of the Colima rift, have been obtained. We recognize fractures and fault zones of local and regional character from their characteristic magnetic anomaly response. Large mapped structures include the north-south Montitlan, northeast-southwest La Lumbre, and east-west La Escondida faults, which can be traced across the area from the magnetic profiles. Fault magnetic anomalies are modeled by lateral contrasts in terms of step models assuming thin dipping elongated zones along the fault planes. The study shows that faults in the CVC volcanic terrain can be investigated by magnetic surveying.

INTRODUCTION

Subsurface structure in volcanic areas has long been investigated by potential field geophysical surveys. Magnetic anomaly studies have been used to investigate magmatic processes and their relationships with deep structure of active volcanoes (e.g., Davis et al., 1983; Nishida and Miyajima, 1984; Sasai et al., 1990; Dzurisin et al., 1990; Connor et al., 1993; Johnston, 1997; Finn et al., 2001). Magnetic methods are well suited for studying volcanoes of intermediate to mafic composition because of the relative abundance of ferromagnetic minerals capable of generating magnetic anomalies (Grant, 1985). The distribution, morphology, and arrangement of magnetic anomalies are often related to characteristics associated with shallow and deep geological structures.

Of particular interest in the study of volcanic complexes is the occurrence of faults, deformation features, and weakness zones, which may be related to the volcanic activity, volcano collapse, volcanic debris avalanches, and hydrothermal and tectonic activity (e.g., Van Wyk de Vries and Francis, 1997; Ventura et al., 1999; Podolsky and Roberts, 2008; Vezzoli et al., 2008). In active volcanic zones, study of faulting may be complicated by resurfacing of faults and features related to fault activity, including drainage patterns by lavas, pyroclasts, or debris avalanches (e.g., Parfitt and Peacock, 2001; Day et al., 2005; Holland et al., 2006; Podolsky and Roberts, 2008). Mapping of faults and investigation of fault characteristics, geometry, propagation, and growth fault histories are critical for understanding volcano-tectonic activity and hazard evaluation.

There are relatively few studies in the literature on magnetic anomalies associated with faults in volcanic sequences. Henkel and Guzman (1977) reported that fault zones are characterized by elongated magnetic minima, associated with oxidation of magnetite to hematite within the fault. They documented lower magnetic susceptibilities and reduction of the intensity of remanent magnetization in the igneous rocks across the fractures. Ozima and Kinoshita (1964) studied the magnetic fabric (measured by anisotropy of magnetic susceptibility) of andesitic rocks across a fault zone, and observed an apparent increase of anisotropy close to the fault zone. Igneous rocks do not show stress-induced effects due perhaps to incompetence under low-temperature and high-pressure conditions. These characteristics have been exploited to infer deformation histories where rocks of

*Corresponding author. Email: juf@geofisica.unam.mx.

Geosphere; February 2010; v. 6; no. 1; p. 35–46; doi: 10.1130/GES00204.1; 11 figures; 2 tables.

varying competence under low strain conditions are present in major deformation zones (e.g., Rathore and Becke, 1980).

In this paper we apply magnetic surveys to investigate faults and subsurface structure in the volcanic terrain of the central and southern sector of the Colima rift and Colima volcanic complex (CVC), western Mexico. The CVC is formed by a volcanic chain oriented north-south that contains three composite volcanoes: Cantaro, Nevado de Colima, and Colima (Fig. 1). The study area includes the Nevado de Colima and Colima volcanoes and extends within and across the southern Colima rift. Colima is the most historically active volcano in Mexico (Robin et al., 1987; Luhr and Carmichael, 1980, 1990; Luhr, 1981; Breton González et al., 2002), and has been extensively studied as part of the International Decade of Volcanic Hazard Reduction. The CVC within the rift has been linked to major fault structures, such as the La Lumbre fault (e.g., Lopez-Loera and Urrutia-Fucugauchi, 1996; Garduño et al., 1998). Study of faults, deformation, and stratigraphy of the CVC and Colima rift has been hampered by the young volcanic avalanches and pyroclastic and volcaniclastic rocks that cover the area. For this study, a network of magnetic profiles was used to investigate the fault system in the volcanic complex and the southern sector of the rift zone (Fig. 2). Our total field magnetic anomaly survey shows that characteristic magnetic anomalies are related to fault zones in the CVC, and that subsurface structures and stratigraphy can be investigated and modeled.

COLIMA VOLCANIC COMPLEX

The CVC is located at the southwestern sector of the Trans-Mexican Volcanic Belt, where the volcanic front is closest to the Middle America Trench (Fig. 1) (Urrutia-Fucugauchi and Del Castillo, 1977; Luhr and Carmichael, 1980, 1990; Rosas-Elguera et al., 1996). Volcanic activity migrated southward during construction of the volcanic complex, and Colima volcano is the only active center at present (Robin et al., 1987). This volcanic complex is located at the south-central sector of a large tectonic graben oriented north-south, ~150 km long and 40 km wide (Luhr and Carmichael, 1990), which defines the Colima rift. The eastern and western margins of the Colima rift are marked by the basins of Tuxpan–El Naranjo and the Armeria Rivers, respectively (Fig. 2). The Colima rift forms part of a major tectonic structure that intersects and forms a rift-rift-rift continental triple junction to the north of the CVC and south of Guadalajara region (Fig. 1), and that has been intensively studied (e.g., Luhr and Carmichael, 1980, 1990; Allan and Carmichael, 1984; Allan, 1986; Urrutia-Fucugauchi and Molina-Garza, 1992; Rosas-Elguera et al., 1996; Rosas-Elguera and Urrutia-Fucugauchi, 1998).

The Colima rift has been considered as the eastern boundary of the Jalisco block; its southern segment has a general orientation that varies north-northeast–south-southwest with respect to its north-south regional trend. The local basement of the CVC (Luhr and Carmichael, 1980, 1990) is formed by volcanic, volcano-sedimentary, and marine sedimentary rocks associated with a magmatic arc. The age of the magmatic arc sequence varies from Neocomian to early Albian (Alencaster and Pantoja-Alor, 1986). Geophysical studies have indicated as much as 900 m of volcaniclastic sediments in the northern sector of the Colima graben (Allan, 1985). In the southern sector of the CVC between Colima volcano and Colima City, sediments may be as thick as 700 m (Lopez-Loera and Gutierrez, 1977). The CVC products are characterized by a series of avalanche debris deposits that create a total volume between 60 and 100 km^3; some of the largest avalanches may have reached distances of ~100 km toward the Pacific coast (Stoopes and Sheridan, 1992; Komorowski et al., 1997).

Reconnaissance studies suggest that fault and fractures affecting the volcanic structures show two dominant orientations: north-south, which coincides with the Cantaro–Nevado de Colima–Colima volcanic alignment (Aubert and Lima, 1986; Lopez-Loera and Urrutia-Fucugauchi, 1996; Rosas-Elguera et al., 1996), and northeast-southwest, which coincides with the alignment of the parasitic cinder cone named Los Volcancitos.

Rock magnetic properties of samples from the summit area of Colima were reported by Connor et al. (1993) and Urrutia-Fucugauchi et al. (1997). Low-field magnetic susceptibilities for five samples from the summit dome and lava flows range between 2.6×10^{-4} and 8.2×10^{-4} SI units. Corresponding data for remanent magnetization intensity yield 1.08–3.84 A/m. Three samples present discrete unblocking temperatures higher than 450 °C to 575 °C, and two samples present a wide and lower range of distributed unblocking temperatures.

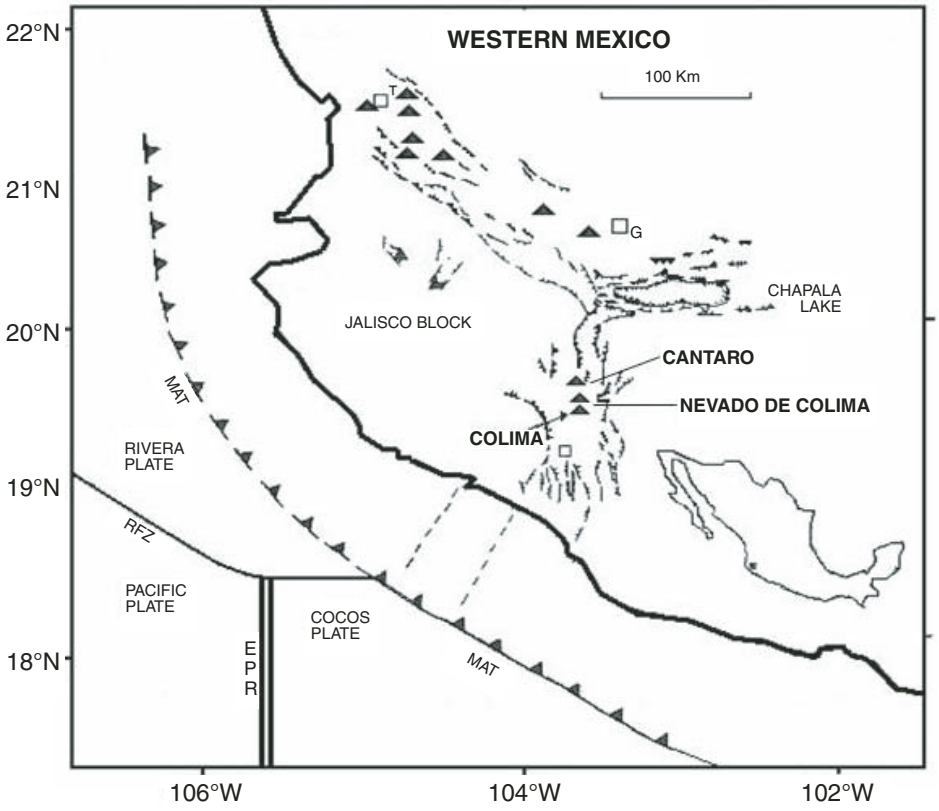

Figure 1. Tectonic map of western Mexico showing the Colima rift and the Colima volcanic complex. Black triangles represent major volcanic centers in the area. Major structural lineaments mark the tectonic depressions of the Colima rift and Tepic–Zacoalco Rifts. G—Guadalajara City; T—Tepic; MAT—Mesoamerican Trench; EPR—East Pacific Rise; RFZ—Rivera fracture zone.

We measured the rock magnetic properties of 50 samples collected along the magnetic transect between Atenquique and El Playon (Fig. 2; profile 1–1′). The intensity and direction of remanent magnetization were measured, as well as low-field magnetic susceptibility (Lopez-Loera and Urrutia-Fucugauchi, 1999). The magnetic properties of the volcanic fragments in the debris avalanche deposits from Nevado de Colima and Colima have wide ranges of variation. Samples from the Nevado de Colima avalanche give low-field magnetic susceptibilities varying between ~3.7 × 10^{-4} and 10.6 × 10^{-4}, with a mean of 7.2 × 10^{-4} SI units. The remanent magnetization intensities vary from 0.55 to 1.86 A/m, with a mean of 1.2 A/m. The susceptibilities and magnetization intensities are associated with magnetic anomaly responses with ranges of 271 nT to −259 nT and horizontal gradients of 0.754 nT/m to −0.932 nT/m. Samples from the younger Colima volcano avalanche deposit show a range for the susceptibility from 1.3 × 10^{-4} to 8.4 × 10^{-4} and mean of 5.4 × 10^{-4} SI, and the remanent intensities range from 0.73 to 3.69 A/m with a mean of 2.52 A/m. The magnetic anomaly response vary between 165 nT and −531 nT and horizontal gradients between 1.196 nT/m and −0.71 nT/m. Andesitic lavas of Nevado de Colima give susceptibility ranging from 2.5 × 10^{-4} to 10 × 10^{-4} SI and mean of 6.2 × 10^{-4} SI, and remanent intensity from 1.35 to 7.33 A/m and a mean of 0.56 A/m. The magnetic anomaly response varies between 277 nT and −430 nT and horizontal gradients vary between 1.13 nT/m and −1.03 nT/m. Samples from historic andesitic lavas in Colima volcano, eastern caldera wall, show susceptibility from 4.2 × 10^{-4} to 9.8 × 10^{-4} SI and a mean of 5.8 × 10^{-4} SI, and remanent intensity ranges from 0.8 to 1.0 A/m; the mean is 0.88 A/m. The magnetic anomaly response ranges from 742 nT to −531 nT and horizontal gradients vary from 1.572 nT/m to −1.174 nT/m.

The magnetic polarity of the andesitic lava flows of Nevado de Colima and Colima is normal, which is consistent with an age within the Brunhes chron for the stratovolcanoes. Directions of the natural remanence for volcanic clasts of the old and young debris avalanche deposits show scattered directional angular distributions (Urrutia-Fucugauchi et al., 1997), suggesting that emplacement occurred at intermediate to low temperatures. An air-fall ash deposit also showed a scattered directional distribution. The vectorial composition and directional stability of samples were investigated by alternating field (AF) and thermal demagnetizations. AF demagnetization was completed with an AF demagnetizer up to maximum fields of 100 nT. Thermal demagnetization was completed in steps up to temperatures of 550–600 °C. Magnetic carriers are members of the titanomagnetite and titanohematite series, with low and intermediate coercivity, and scattered and definite unblocking temperature spectra. In general, samples show high magnetic stability upon AF and thermal demagnetization, with mainly univectorial or in some cases multicomponent magnetizations. Unblocking temperatures for some samples are in the range 500–575 °C, characteristic of magnetite and Ti-poor titanomagnetites.

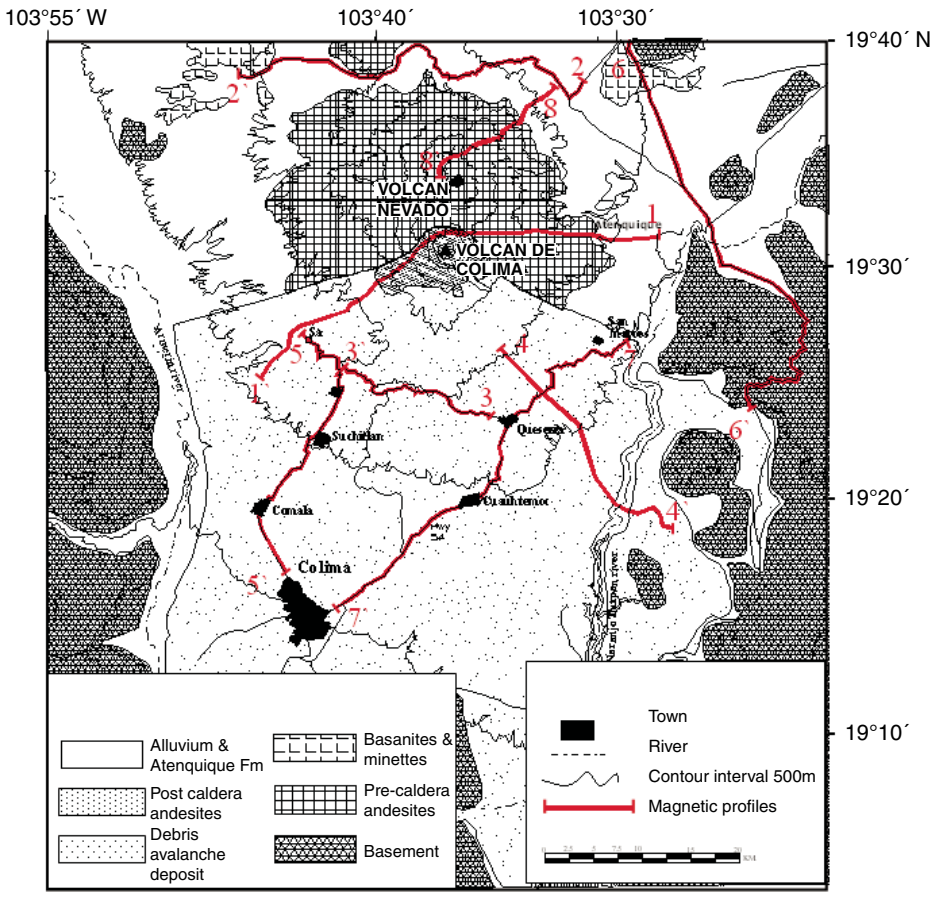

Modified from Luhr and Carmichel, 1990

Figure 2. Geologic map of the Colima volcanic complex and the locations of the eight magnetic profiles (see text and Table 1 for information on profiles).

MAGNETIC ANOMALY FIELD DATA

The magnetic surveys in the CVC were conducted via a network of profiles crossing the major structural features of the volcanoes and Colima rift boundaries represented by the north-south–trending normal faults of the rift. The magnetic field observations were completed along 284.5 km distributed in 8 magnetic profiles with stations spaced every 0.5 km (Fig. 2). Diurnal geomagnetic variation effects have been registered at two base stations in the study area with Geometrics G-826 and G-856 proton-precession magnetometers (http://www.austinex.com/mag801.htm). We calculated the total magnetic field residual for all profiles using a least-squares linear fit regional. We applied a low-pass filter to remove high-frequency shallow effects, to enhance effects of the subsurface structure. Profile data are summarized in Table 1 (see Fig. 2). Magnetic field measurements were taken across inferred traces of major faults mapped in the region. Some faults show topographic expression, recognized from the basin drainage pattern constructed in the volcano-sedimentary deposits.

The largest anomalies observed in the magnetic profiles correspond to the inferred and mapped fault zones. The large structures mapped in the geologic surveys include the Montitlan, La Lumbre, and La Escondida faults. The fault zones show characteristic anomalies, which show larger amplitudes and distinct wavelengths with respect to the anomalies on the volcaniclastic terrain. Results of the characteristic magnetic anomalies over the fault traces are summarized in Figures 3, 4, and 5. The description of the

magnetic anomaly over the surface trace along the profiles is given in the following. The characteristic anomalies for the three largest faults and the different patterns in terms of amplitude and wavelength can be observed in the magnetic anomaly profiles. The differences are related to fault zone characteristics, magnetic susceptibility lateral contrasts across the fault zones, and volcaniclastic cover. This is examined from the forward models for the profiles in the following section. The eastern limit of the Colima rift, marked by the Tuxpan-Naranjo river basin, is similarly characterized by a magnetic anomaly. The Montitlan fault trends almost north-south across the western slope of Colima volcano. The trace of the fault is inferred from the magnetic anomalies in profile 1–1′ (Salsipuedes–El Playon–Atenquique), profile 2–2′ (El Penal–Floripondio–Ciudad Guzman) and profile 3–3′ (La Zacatera–Montitlan–Queseria) (Fig. 3). The La Escondida fault trends east-west across the Colima rift, south of Colima volcano on the debris avalanche terrain, and its surface trace is marked in profile 4–4′ (El Fresnal–Tonila), profile 5–5′ (El Tecuan–San Antonio–Villa de Alvarez) and profile 6–6′ (Ciudad Guzman–4 Caminos–Llanitos) (Fig. 4). The La Lumbre fault has a northeast-southwest trend and a well-marked surface expression affecting the south flank of Colima volcano, and its surface trace is constrained from profile 5–5′, profile 1–1′, and profile 6–6′ (Fig. 5).

The magnetic anomaly over the fault zones appears well defined, marked by sharp short-wavelength minima, which could be related to alteration along weakness planes in the volcanic and volcaniclastic deposits. Fault characteristics and associated magnetic anomalies are discussed here for the Montitlan, La

TABLE 1. SUMMARY OF MAGNETIC ANOMALY PROFILES IN THE COLIMA VOLCANIC COMPLEX

Magnetic profiles	Coordinates (long, °W; lat, °N) Start	End	Length (km)	Orientation	Surface geology	Faults
1-1′	103.798	103.499	64			
Salsipuedes–El Playon–Atenquique	19.4207	19.5249		SW-NE W-E	Qaf, Qca-Qcb, Qna, Qaf	Montitlan La Lumbre
2–2′	103.824	103.486	27.5			
El Penal–Floripondio–Ciudad Guzman	19.691	19.6674		W-E	Qbm, Qna, Qaf	Montitlan
3–3′	103.733	103.578	24			
La Zacatera–Montitlan–Queseria	19.4557	19.3885		W-E	Qav	La Lumbre No Name Montitlan
4–4′	103.609	103.451	38.5			
El Fresnal–Tonila	19.4959	19.3291		SE-NW	Qav	Naranjo River La Escondida
5–5′	103.744	103.705	37.5			
El Tecuan–San Antonio–Villa de Alvarez	19.2840	19.4775		S-N	Qav	La Lumbre La Escondida
6–6′	103.396	103.494	47.9			
Ciudad Guzman –4 Caminos–Llanitos	19.4096	19.8241		NW-SE	Qaf, Qbm	La Lumbre Naranjo River La Escondida
7–7′	103.689	103.509	29			
Colima–San Marcos	19.2379	19.4258		SW-NE	Qav	La Escondida
8–8′	103.631	103.533	12.5			
Nevado Antenas–Camino Grullo–Ciudad Guzman	19.5664	19.6292		SW-NE	Qnc, Qnb, Qna, Qaf	Three caldera faults with no name

Note: Surface geology after Luhr and Carmichael (1980, 1990). Units: Qcb—postcaldera andesitic lavas and breccias from Volcan de Colima; Qav—volcanic debris avalanche deposit from collapse of ancestral Volcan de Colima; Qbm—lavas and scoriae of basanite to minette composition erupted from cinder cones; Qnc—postcaldera andesitic lavas and breccias from Nevado de Colima, covered by younger ash- and scoria-fall deposits in many places; Qca—precaldera andesitic lavas and breccias from Volcan de Colima, covered by younger ash- and scoria-fall layers in many places; Qnb—precaldera (Stage II) andesitic lavas and breccias from Nevado de Colima, covered by younger ash- and scoria-fall layers in many places; Qaf—Atenquique Formation, volcaniclastics and gravel derived from Colima volcanoes; Qna—precaldera (Stage I) andesitic lavas and breccias from Nevado de Colima, covered by younger ash- and scoria-fall layers in many places; Qaln—andesitic lavas from Nevado; Qalc—andesitic lavas from Colima; Tb—igneous, metaigneous, and clastic sedimentary rocks; Cz—Cretaceous limestones. W—west; E—east; S—south; N—north; SE—southeast; SW—southwest; NW—northwest; NE—northeast.

Escondida, and La Lumbre faults. Modeling of magnetic anomaly profiles is carried out assuming step models and thin elongated dike-like narrow zones, simulating weakness zones along fault planes.

Montitlan North-South Fault

The deformation and weakness zone that define this fault have been considered to be associated with the CVC. The zone extends from Cantaro to Nevado and Colima volcanoes up to the Los Hijos del Volcan cones at the southern sector of Colima volcano. This fault has been inferred from geological mapping surveys (Rosas-Elguera et al., 1996) and apparently marked in a study of self-potential anomalies at the El Playon area (Aubert and Lima, 1986).

Fault surface trace has been interpreted in three of the magnetic profiles that have an east-west orientation (Fig. 3). In profile 2–2′, we interpreted the fault as a magnetic low with amplitude of ~850 nT. In profile 1–1′, which crosses Colima volcano (Salsipuedes-Atenquique), the fault is identified with a magnetic anomaly of >1800 nT. In profile 3–3′ the fault is identified by magnetic anomaly amplitudes of ~379 nT. The magnetic total intensity values where the fault is identified show large contrasts, which may be associated with the thickness of the volcanic deposits located across the profiles. In profile 2–2′, the lavas and breccias of Nevado de Colima are covered by several dozens of meters thickness of young ash- and scoria-fall layers, whereas in the crossing with profile 1–1′, these volcanic products are not as thick. Profile 3–3′ shows thicknesses between 500 and 700 m, according to cross-section layer models of a resistivity study (carried out by Lopez-Loera and Gutierrez, 1977). Komorowski et al. (1997), on the basis of radiometric dating, suggested the presence of at least 12 different avalanches. That is a possible explanation for the great thickness identified in the avalanche deposits toward the south of Colima volcano.

La Escondida East-West Fault

This fault has an inferred east-west orientation and is located toward the southern part of Colima volcano. Its apparent trace is suggested from Tuxpan-Naranjo river toward the proximities of Armería River. Characteristic anomalies related to the fault have been identified in three

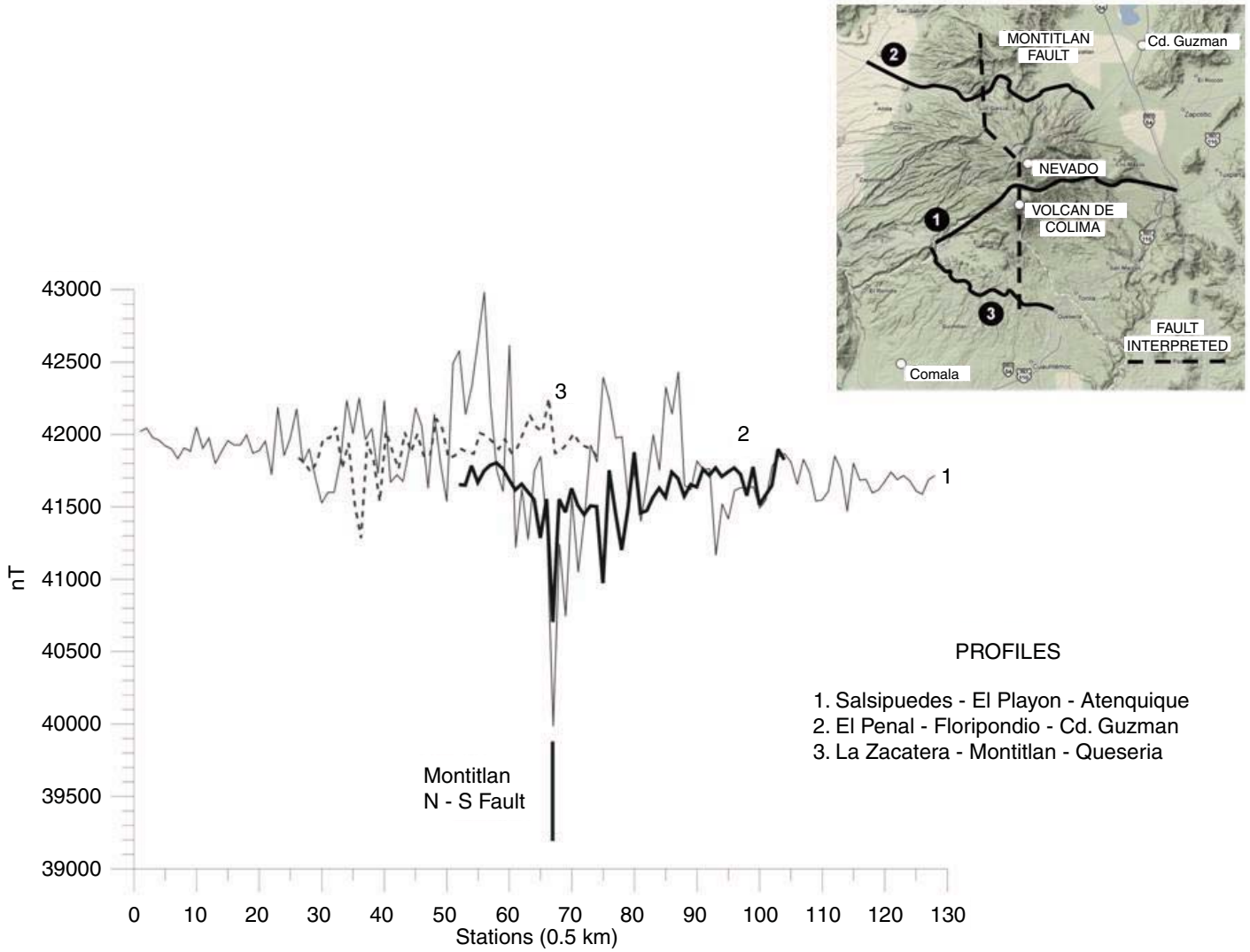

Figure 3. Total field magnetic anomalies observed over the north-south–trending Montitlan fault zone. Diagram shows the anomalies observed in three profiles of general orientation west-east: profile 1–1′, profile 2–2′, and profile 3–3′. Relative positions of profiles and inferred trends of fault zone are given in the inset.

of the magnetic profiles. In profile 6–6′, located toward the east of Colima volcano, a weakness zone associated with the fault is identified with an anomaly generated by a magnetic low with an amplitude of ~487 nT. In profile 4–4′, south-southeast of Colima volcano, the fault trace is interpreted to be associated with an anomaly characterized by amplitudes of ~676 nT. In magnetic profile 5–5′, southwest of Colima volcano, the fault trace is marked by a magnetic anomaly with an amplitude of ~745 nT.

La Lumbre Southwest-Northeast Fault

This fault crosses the summit area of Colima volcano with a southwest-northeast strike. Its inferred trace extends for more than 100 km, from the Manzanillo area at the Pacific Ocean margin to Colima volcano. It was mapped in Lopez-Loera and Urrutia Fucugauchi (1996), and later referred to as the Tamazula fault by Garduño et al. (1998) as part of a regional geological mapping project. We interpret the fault trace in three of the magnetic profiles in the CVC area. In profile 1–1′ (east-west orientation that crosses the summit area of Colima volcano), the fault zone shows a magnetic anomaly of ~745 nT. In profile 5–5′ (north-south orientation), the fault trace can be identified by a magnetic anomaly of ~670 nT. In profile 6–6′ (northwest-southeast orientation), the fault trace is inferred from a magnetic anomaly with an amplitude of ~368 nT.

MAGNETIC ANOMALY MODELING

The geometry and the magnetic properties of the sources associated with the anomalies are modeled using the GM-SYS software (the GM-SYS inversion routine utilizes a Marquardt inversion algorithm; Marquardt, 1963) to linearize and invert the calculations. GM-SYS uses an implementation of this algorithm for magnetic data processing developed by the U.S. Geological Survey in the computer program SAKI (Webring, 1985). The anomalies are modeled by polygonal bodies with different magnetizations. A major limitation in the analysis is the lack of information concerning magnetic property variations with depth. A problem in constructing quantitative models is the heterogeneity of magnetic properties observed in the volcaniclastic and debris avalanche deposits, where remanent magnetizations reside in volcanic clasts, producing scattered magnetization directions of varying intensity. Large variations in magnetic susceptibility and remanence intensity result

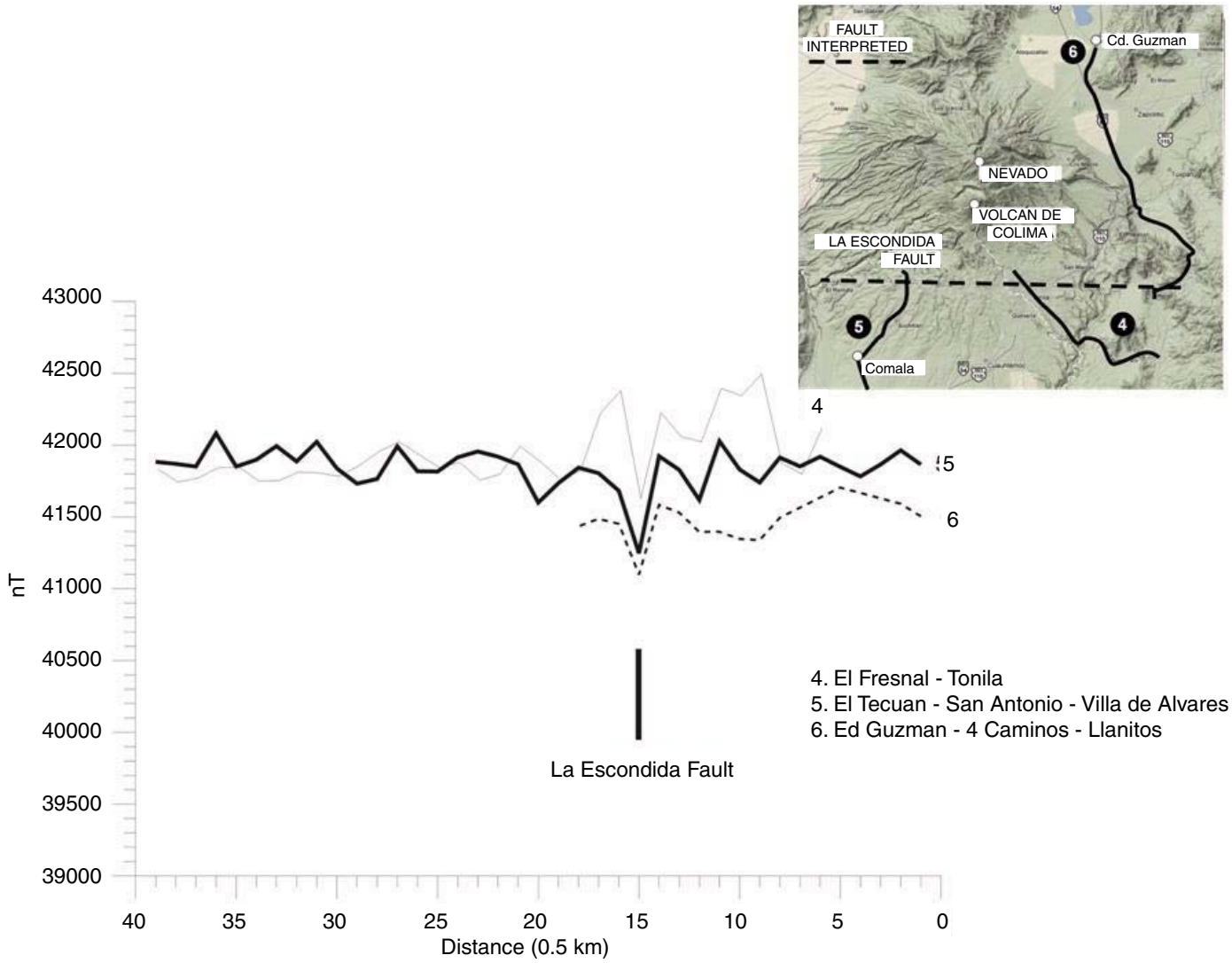

Figure 4. Total field magnetic anomalies observed over the east-west–trending La Escondida fault zone. Diagram shows the anomalies observed in profiles 4–4′, 5–5′ and 6–6′. Relative positions of profiles and inferred trends of fault zone are given in the inset diagram.

from hydrothermal alteration and weathering along fault planes. The shape of magnetic anomalies is dependent on relative orientations of the magnetization vector and geometry of the fault plane. Magnetic field contributions from the surrounding units are also vectorially added to the magnetic field at the surface. Samples for rock magnetic studies were obtained for different lithological units: andesitic flows and breccias, pyroclastic deposits, and volcanic debris avalanches (Connor et al., 1993; Urrutia-Fucugauchi et al., 1997; this work). Averages for the magnetic susceptibilities and intensity and direction of remanent magnetization have been used as initial values for the modeling. The initial models for the profiles are constructed based on the geological mapping and cross sections in Luhr and Carmichael (1980, 1990) and Alencaster and Pantoja-Alor (1986). Geological units correspond to debris avalanche deposits (Qav), postcaldera andesitic lavas and breccias (Qcb), basanite to minette lavas and scoria from cinder cones (Qbm), Nevado de Colima postcaldera andesitic lavas and breccias (Qnc), Colima precaldera andesitic lavas and breccias (Qca), Nevado de Colima stage II andesitic lavas and breccias (Qnb), volcanic siliciclastics and gravels of the Atenquique Formation (Qaf), Nevado de Colima precaldera stage I andesitic lavas and breccias (Qna), andesitic lavas from Colima (Qalc), andesitic lavas from Nevado (Qaln), igneous and clastic sedimentary rocks (Tb), and a Cretaceous limestone sequence (Cz). Profile data are summarized in Table 1. Most units are covered by young ash-fall and scoria deposits. The faults in the CVC volcanic terrains show magnetic minima (Figs. 3–5) that characterize the fault zones.

Magnetic anomalies observed over fault zones have been modeled by lateral contrasts of magnetization using the step model (Grant and West, 1965). Initially we modeled the CVC magnetic anomalies using step geometries, cutting the volcanic units with different inclinations for fault planes cutting the sequences. Although calculated anomalies were fitted to observed anomalies, potential problems in interpretation of the step fault models result from relatively small contrasts in lateral physical properties and lack of resolution in vertical extent of faults. Faults may generally affect

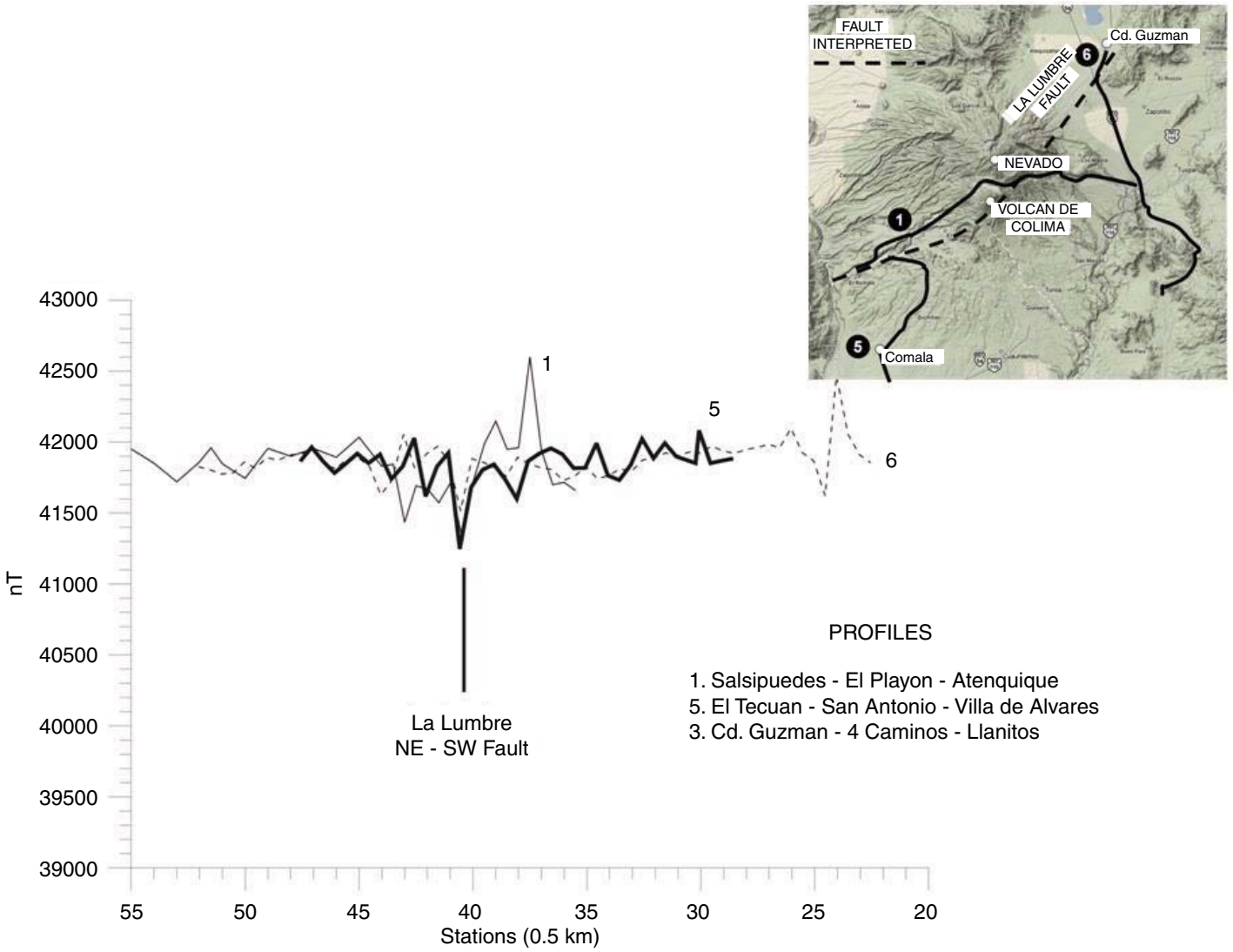

Figure 5. Total field magnetic anomalies observed over the northeast-southwest–trending La Lumbre fault zone. Diagram shows the anomalies observed in profiles 1–1′, 5–5′, and 6–6′. Relative positions of profiles and inferred trends of fault zone are given in the inset diagram.

rock sequences, resulting in juxtaposition of units with different magnetic properties across fault zones, giving magnetic anomalies (e.g., Grant, 1985; Grant and West, 1965). In the CVC volcano-sedimentary terrains with thick volcaniclastic and avalanche deposits, normal faulting set the same rock type in contact within the debris avalanche deposits and no lateral contrasts. In volcanic areas weakness zones associated with fractures and/or faults are common (Day et al., 2005; Holland et al., 2006; Vezzoli et al., 2008). When rain and surface waters get underground (percolation) and are in contact with fractures and fault planes, ferromagnesian minerals oxidize, reducing their susceptibility and magnetic intensity, and creating an appearance of magnetic lows aligned with fault trends (Ozima and Kinoshita, 1964; Henkel and Guzman, 1977; Lopez-Loera and Urrutia-Fucugauchi, 1999).

The CVC magnetic anomalies are modeled using step geometries and thin elongated dipping bodies along the fault planes. Model parameters are summarized in Table 2.

TABLE 2. SUMMARY OF MAGNETIC PARAMETERS USED IN THE MODELS

Units	Magnetic susceptibility SI (10^{-4})	Remanence Intensity (A/m)	Inc	Dec	Geology
Profile 1–1′ Salsipuedes–El Playon–Atenquique					
Qca	1.0	1.8	46	10	Precaldera andesitic lavas and breccias from Volcan de Colima
Qcb	7.0	7.7	50	30	Postcaldera andesitic lavas and breccias from Volcan de Colima
Qna	0.5	7.33	23	10	Precaldera (Stage I) andesitic lavas and breccias from Nevado de Colima
Qalc	0.6	1.5	50	10	Lavas from Volcan de Colima
Qaln	5.0	7.3	60	140	Andesitic lavas from Nevado de Colima
Fault (f_M)	0.1	0.4	22	100	Montitlan fault
Fault (f_{LL})	0.1	4.0	90	10	La Lumbre fault
Profile 2–2′ El Penal–Floripondio–Ciudad Guzman					
Qaf_w	0.03	5.0	61	20	West Atenquique Formation lavas
Qbm	3.0	0.1	52	10	Lavas and scoria of basanite
Fault (f_M)	0.1	0.4	20	20	Montitlan fault
Qna	13.0	0.4	67	60	Precaldera andesitic and lavas from Nevado de Colima
Qaf_E	0.01	1.0	7	120	East Atenquique Formation pyroclasts
Tb	9.0	0.5	16	10	Igneous, metaigneous, and clastic sedimentary rocks
Cz	0	0			Limestone
Profile 3–3′ La Zacatera–Montitlan–Queseria					
Qav	44.0	0.6	16	30	Colima volcanic debris avalanche
Fault (f_{LL})	0.1	0.05	46	10	La Lumbre fault
Fault (f_C)	0.03	0.005	46	10	Central fault
Fault (f_M)	0.1	0.4	23	40	Montitlan fault
Cz	0	0			Limestone
Profile 4–4′ El Fresnal–Tonila					
Qav_S	9.5	0.6	49	10	Colima volcanic debris avalanche
Fault (f_N)	0.01	0.3	35	70	El Naranjo River fault
Qav_C	7.5	1.4	39	20	Colima volcanic debris avalanche
Fault (f_{Es})	0.01	0.4	42	46	La Escondida fault
Qav_N	94.0	1.5	7	20	Colima volcanic debris avalanche
Cz	0	0			Limestone
Profile 5–5′ El Tecuan–San Antonio–Villa de Alvarez					
Qav	80.0	5.9	16	30	Colima volcanic debris avalanche
Fault (f_{LL})	10.0	3.8	46	10	La Lumbre fault
Fault (f_{Es})	0.01	0.8	43	40	La Escondida fault
Cz	0	0			Limestone
Profile 6–6′ Ciudad Guzman–4 Caminos–Llanitos					
Qaf	1.6	5.5	87	17	Atenquique Formation lavas
Fault (f_{LL})	0.1	4.0	47	17	La Lumbre fault
Qbm	84.0	5.7	24	10	Lavas and scoria of basanite erupted from cinder cones
Fault (f_N)	0.2	0.5	17	110	El Naranjo River fault
Fault (f_{NN})	0.1	0.1	46	10	Fault
Fault (f_{ES})	0.01	0.5	10	70	La Escondida fault
Tb	10.0	1.9	13	10	Igneous and clastic sedimentary rocks
Cz	0	0			Limestone

Note: Inc—inclination; Dec—declination.

Results of the modeling for the Montitlan fault in profiles 1–1′, 2–2′, and 3–3′ are shown in Figures 6, 7, and 8, respectively. Models for the La Escondida fault in profiles 4–4′, 5–5′, and 6–6′ are shown in Figures 9, 10, and 11. Models for the La Lumbre fault in profiles 1–1′, 3–3′, and 6–6′ are shown in Figures 6, 8, and 11. In most cases vertical or near-vertical fault planes have been initially assumed; dips of plane were then modified to obtain a tighter fit of calculated anomalies. For the modeling, varying widths for the fault zones were tested to obtain fit to observed anomalies. These estimates were influenced by the lateral contrasts arising from the fault displacements assumed and the geometry of the volcanic units, which were not constrained independently. Modeling allows evaluating varying width with depth for the fault zones, keeping as constraints a tighter fit to observed anomalies. Faults that do not apparently present large lengths across the Colima rift area are also characterized in the profiles and models. These faults include fault fn in profile 3–3′ and fault fn in profile 6–6′. Anomalies with larger wavelengths may be associated with fault zones covered by younger volcanic deposits or deeper lateral susceptibility contrasts. This can be observed for the larger fault zones of Montitlan, La Lumbre, and La Escondida, and other faults inferred in

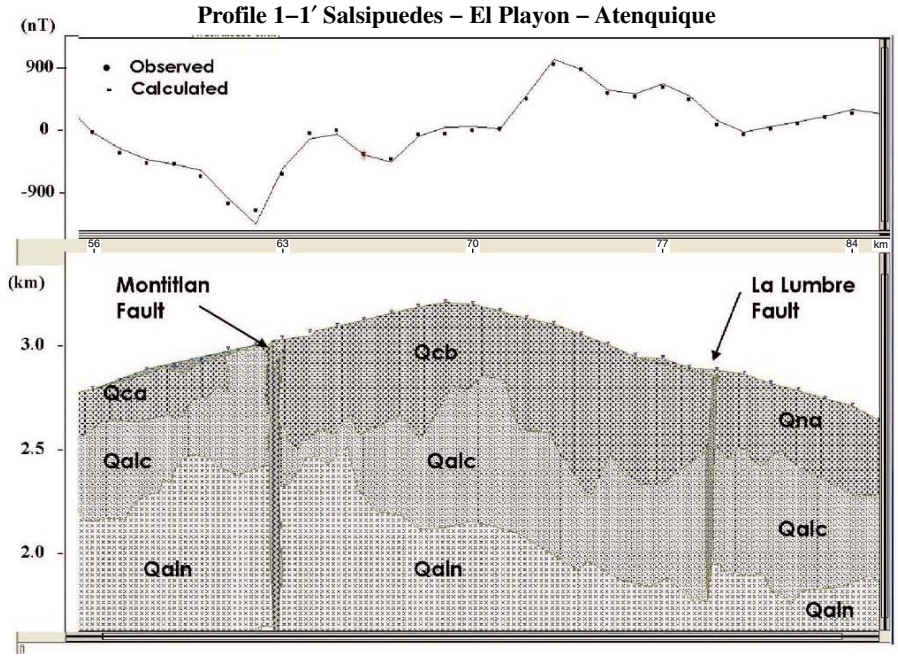

Figure 6. Model for magnetic profile 1–1′. Top: Observed and calculated magnetic anomalies. Bottom: Magnetic model. Observed anomalies correspond to residual magnetic field (RMF) and after low-pass filter on RMF data. RMF data were calculated after removal of diurnal variation effects and International Geomagnetic Reference Field. Faults in section are La Lumbre fault. Magnetic parameters used in models are summarized in Table 2. Symbols: Qcb—postcaldera andesitic lavas and breccias from Colima; Qna—precaldera (stage I) andesitic lavas and breccias from Nevado; Qca—precaldera andesitic lavas and breccias from Colima, covered by ash and scoria in places; Qalc—andesitic lavas and pyroclasts from Colima; Qaln—andesitic lavas from Nevado.

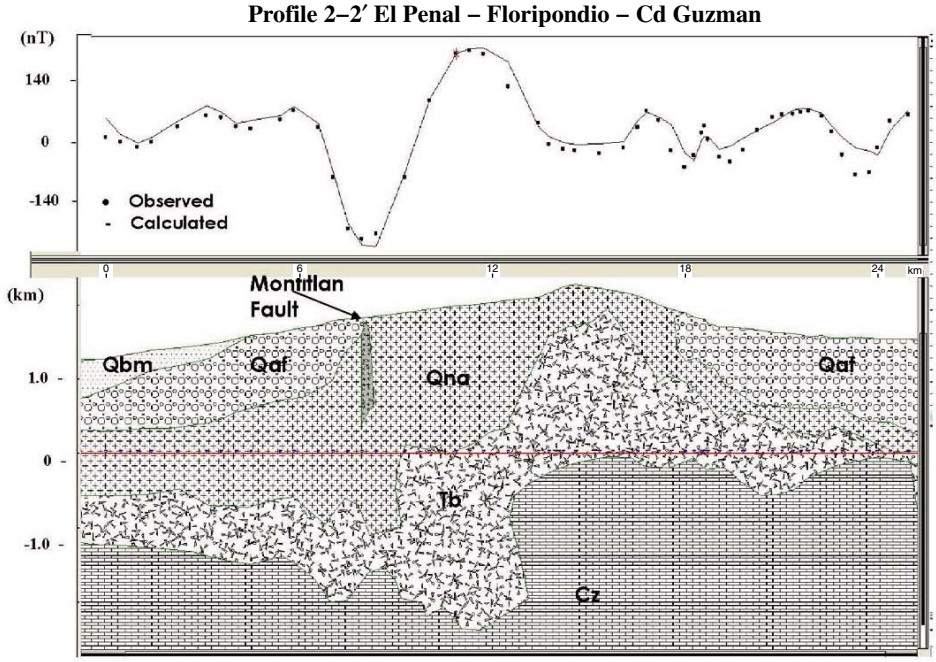

Figure 7. Model for magnetic profile 2–2′. Top: Observed and calculated magnetic anomalies. Bottom: Magnetic model. Observed anomalies correspond to residual magnetic field (RMF) and after low-pass filter on RMF data. RMF data calculated after removal of diurnal variation effects and International Geomagnetic Reference Field. Faults in the section are Montitlan fault. Magnetic parameters used in models are summarized in Table 2. Symbols: Qna—precaldera (stage I) andesitic lavas and breccias from Nevado; Qaf—Atenquique Formation, volcaniclastics and gravel derived from Colima; Qbm—lavas and scoria of basanite to minette composition erupted from cinder cones; Cz—Cretaceous limestone sequence; Tb—igneous, metaigneous, and clastic sedimentary rocks.

the magnetic anomaly modeling. This has been incorporated in the models for the different profiles, where it can be compared to the magnetic response of inferred buried fault zones. Models present lower resolution in terms of estimation of vertical extent of model sources, a limitation in polygonal models. Therefore, the vertical extent of fault planes is not constrained by the magnetic modeling.

CONCLUSIONS

The magnetic anomaly survey over the volcanic terrain in the Colima rift is useful to investigate the volcano-sedimentary units from the Colima volcanic complex. Characteristic magnetic anomalies are observed over the fault zones in the volcanic terrains of the CVC. We draw the following conclusions from our study.

1. The volcanic terrains covered by products of Colima volcanic complex are characterized by several fracture and/or fault zones. Resurfacing due to the thick volcaniclastic lavas, debris avalanche deposits, and pyroclastic deposits obscures the structural features and stratigraphic relationships.

2. Fault zones are shown to be associated with magnetic anomaly minima, which characterize

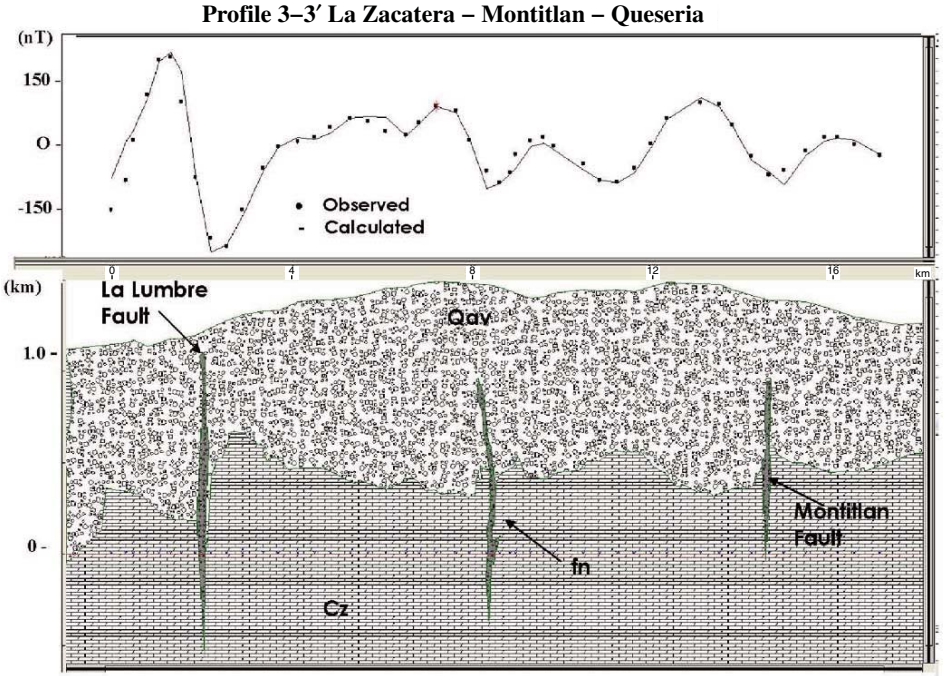

Figure 8. Model for magnetic profile 3–3′. Top: Observed and calculated magnetic anomalies. Bottom: Magnetic model. Observed anomalies correspond to residual magnetic field (RMF) and after low-pass filter on RMF data. RMF data calculated after removal of diurnal variation effects and International Geomagnetic Reference Field. Faults in section are La Lumbre, Montitlan, and an unnamed fault referred to as fn. Magnetic parameters used in models are summarized in Table 2. Symbols: Qav—volcanic debris avalanche deposit from the collapse of ancestral Colima; Cz—Cretaceous limestone sequence.

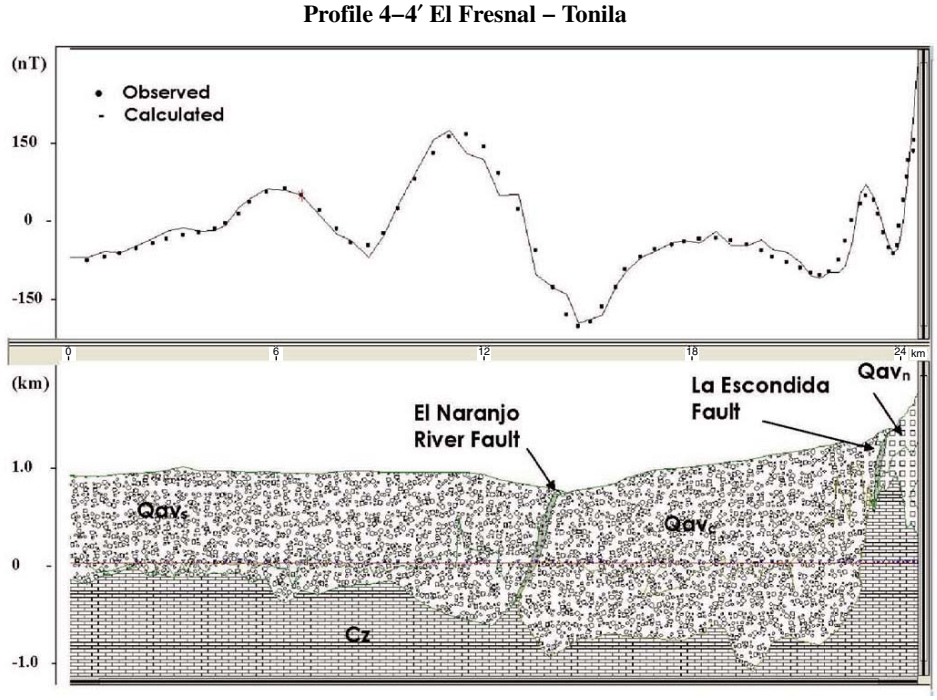

Figure 9. Model for magnetic profile 4–4′. Top: Observed and calculated magnetic anomalies. Bottom: Magnetic model. Observed anomalies correspond to residual magnetic field (RMF) and after low-pass filter on RMF data. RMF data calculated after removal of diurnal variation effects and International Geomagnetic Reference Field. Faults in the section are La Escondida and Naranjo River. Magnetic parameters used in models are summarized in Table 2. Symbols: Qav—volcanic debris avalanche deposit from the collapse of ancestral Colima, separated for modeling purposes due to the heterogeneity of the avalanche deposits into southern deposits (Qavs), central deposits (Qavc), and northern deposits (Qavn); Cz—Cretaceous limestone sequence.

the surface fault traces of the La Lumbre, Montitlan, and La Escondida faults (see Figs. 3, 4, and 5).

3. The Montitlan and La Lumbre faults form a fault system that bisects Colima volcano, and appear to be related to deformation and avalanche events in the volcanic edifice.

4. Magnetic anomalies over the fault zones are modeled assuming step fault models and thin elongated zones along the fault planes, surrounded by the volcaniclastic rocks with distinct magnetic susceptibilities and remanent magnetization intensities (Figs. 7–11).

5. Magnetic anomalies over the fault zones were initially modeled using step fault models only, although this type of model shows low resolution in terms of geometric constraints due to relatively small lateral contrasts in magnetic properties.

6. Large variations in magnetic susceptibility and remanence intensity are found in the avalanche and volcaniclastic products. These variations result mainly from the relative contributions of clasts and matrix, and the effects of hydrothermal alteration and weathering.

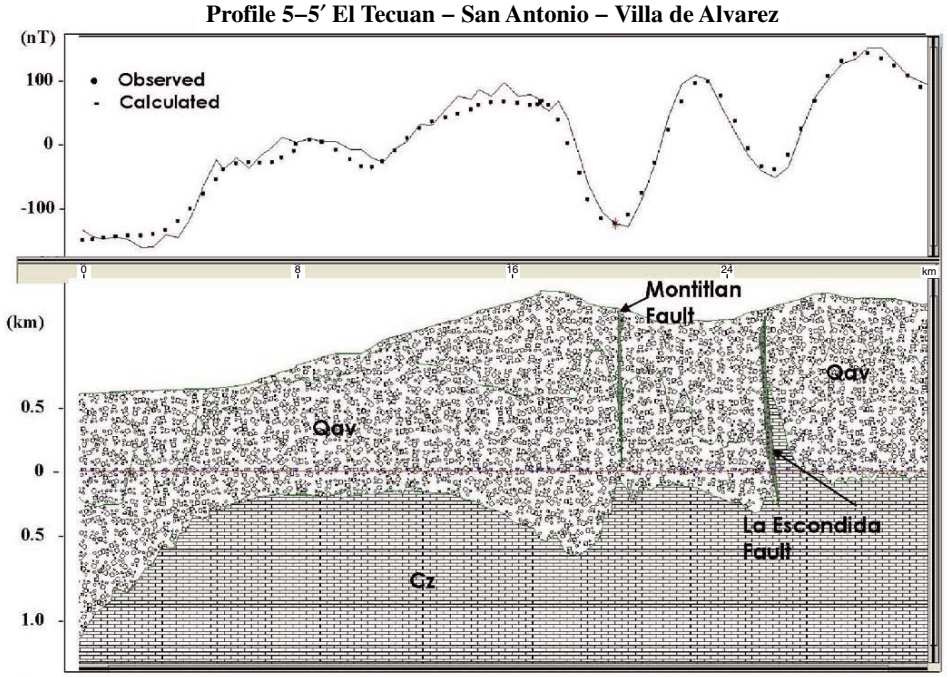

Figure 10. Model for magnetic profile 5–5′. Top: Observed and calculated magnetic anomalies. Bottom: Magnetic model. Observed anomalies correspond to residual magnetic field (RMF) and after low-pass filter on RMF data. RMF data calculated after removal of diurnal variation effects and International Geomagnetic Reference Field. Faults in the section are La Lumbre and La Escondida. Magnetic parameters used in models are summarized in Table 2. Symbols: Qav—volcanic debris avalanche deposit from collapse of ancestral Colima; Cz—Cretaceous limestone sequence.

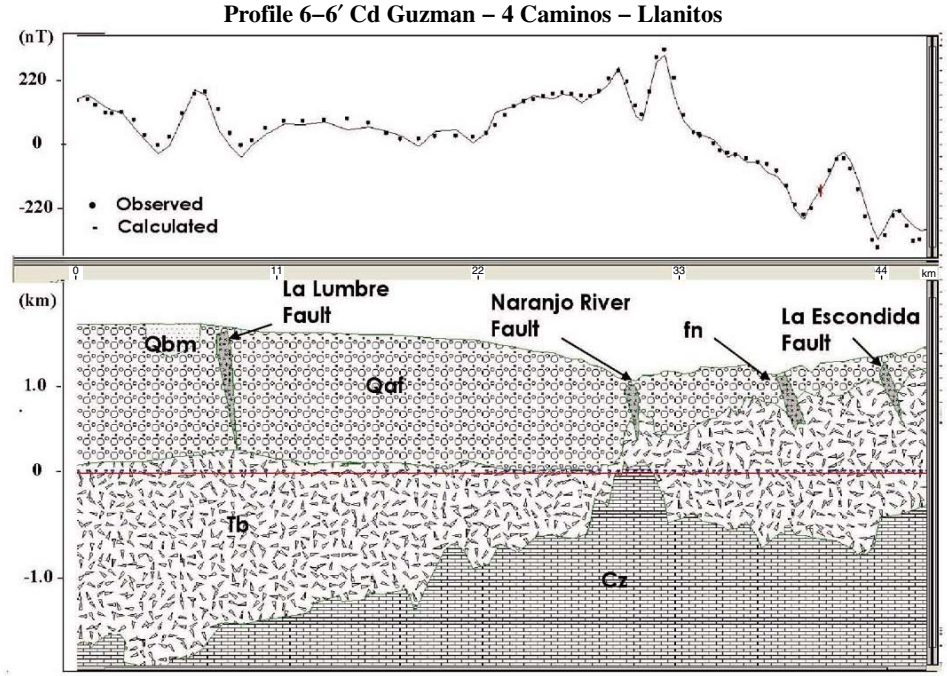

Figure 11. Model for magnetic profile 6–6′. Top: Observed and calculated magnetic anomalies. Bottom: Magnetic model. Observed anomalies correspond to residual magnetic field (RMF) amplitude and after low-pass filter on RMF data. RMF data calculated after removal of diurnal variation effects and International Geomagnetic Reference Field. Faults in section are La Lumbre, La Escondida, Naranjo, and fn, an unnamed fault. Magnetic parameters used in models are summarized in Table 2. Symbols: Qaf—Atenquique Formation, volcaniclastics and gravel derived from Colima; Qbm—basaltic lavas and scoria of basanite to minette composition erupted from cinder cones; Cz—Cretaceous limestone sequence; Tb—igneous, metaigneous, and clastic sedimentary rocks.

ACKNOWLEDGMENTS

This project has been supported by grants and a scholarship for Ph.D. studies from Consejo Nacional de Ciencia y Tecnología (CONACYT) to Lopez-Loera and from UNAM (Universidad Nacional Autonoma de México), PAPIIT (Programa de Apoyo a Proyectos de Investigación e Innovación Tecnológica)-DGAPA (Dirección General de Asuntos del Personal Académico) project IN-102897 and CONACYT project 42682F. We thank David E. Torres-Gaytan for his collaboration in the preparation of graphs. We gratefully acknowledge comments and useful suggestions on earlier versions of the paper by the editor and journal reviewers. The comments resulted in major changes in modeling and data analysis and improvement of the paper.

REFERENCES CITED

Alencaster, G., and Pantoja-Alor, J., 1986, *Coalcomana ramosa* (Boehm) (Bivalvia-ippurtacea) del Albiano temprano del Cerro de Tuxpan, Jalisco: Boletín de la Sociedad Geológica Mexicana, v. 47, p. 33–46.

Allan, J.F., 1985, Sediment depth in northern Colima graben from 3-D interpretation of gravity: Geofísica Internacional, v. 24, p. 21–30.

Allan, J.F., 1986, Geology of the northern Colima and Zacoalco grabens, southwest Mexico: Late Cenozoic rifting in the Mexican volcanic belt: Geological Society of America Bulletin, v. 97, p. 473–485, doi: 10.1130/0016-7606(1986)97<473:GOTNCA>2.0.CO;2.

Allan, J.F., and Carmichael, I.S.E., 1984, Lamprophyric lavas in the Colima graben SW Mexico: Contributions to Mineralogy and Petrology, v. 88, p. 203–216, doi: 10.1007/BF00380166.

Aubert, M., and Lima, E., 1986, Hydrothermal activity detected by self-potential Colima and Volcan de Colima (Mexico): Geofísica Internacional, v. 25, p. 575–586.

Breton González, M., Ramirez-Ruiz, J.J., and Navarro-Ochoa, C., 2002, Summary of the historical eruptive activity of Volcán de Colima, Mexico 1519–2000: Journal of Volcanology and Geothermal Research, v. 117, p. 21–46, doi: 10.1016/S0377-0273(02)00233-0.

Connor, C.B., Lane, S.B., and Clement, B.M., 1993, Structure and thermal characteristics of the summit dome, March, 1990–March, 1991: Volcan de Colima, Mexico: Geofísica Internacional, v. 32, p. 643–657.

Davis, P.M., Pierce, D.R., Mcpherron, R.L., Dzurisin, D., Murray, T., Johnston, M.J.S., and Muller, R., 1983, A volcanomagnetic observation on Mount St. Helens, Washington: Geophysical Research Letters, v. 11, p. 225–228.

Day, S.J., Watts, P., Grilli, S.T., and Kirby, J.T., 2005, Mechanical models of the 1975 Kalapana, Hawaii earthquake and tsunami: Marine Geology, v. 215, p. 59–92, doi: 10.1016/j.margeo.2004.11.008.

Dzurisin, D., Denlinger, R.P., and Rosenbaum, J.G., 1990, Cooling rate and thermal structure determined from progressive magnetization of the dacite dome at Mount St. Helens, Washington: Journal of Geophysical Research, v. 95, p. 2763–2780, doi: 10.1029/JB095iB03p02763.

Finn, C.A., Sisson, T.W., and Ceszcz-Pan, A.M., 2001, Aerogeophysical measurements of collapse-prone hydrothermally altered zones at Mount Rainier volcano: Nature, v. 409, p. 600–603, doi: 10.1038/35054533.

Garduño, V.H., Saucedo, R., Jimenez, Z., Gavilanes, J.C., Cortés, A., and Uribe-Cifuentes, R.M., 1998, La falla Tamazula, limite suroriental del bloque Jalisco y sus relaciones con el complejo volcánico de Colima, México: Revista Mexicana de Ciencias Geologicas, v. 15, p. 132–144.

Grant, F.S., 1985, Aeromagnetics, geology and ore environments, I. Magnetite in igneous, sedimentary and metamorphic rocks: An overview: Geoexploration, v. 23, p. 303–333, doi: 10.1016/0016-7142(85)90001-8.

Grant, F.S., and West, G.F., 1965, Interpretation theory in applied geophysics: International Series in the Earth Sciences: New York, McGraw-Hill, 583 p.

Henkel, H., and Guzman, M., 1977, Magnetic features of fracture zones: Geoexploration, v. 15, p. 173–181, doi: 10.1016/0016-7142(77)90024-2.

Holland, M., Urai, J.L., and Martel, S., 2006, The internal structure of fault zones in basaltic sequences: Earth and Planetary Science Letters, v. 248, p. 286–300, doi: 10.1016/j.epsl.2006.05.035.

Johnston, M.J.S., 1997, Review of electric and magnetic fields accompanying seismic and volcanic activity: Surveys in Geophysics, v. 18, p. 441–475, doi: 10.1023/A:1006500408086.

Komorowski, J.C., Navarro, C., Cortés, A., Saucedo, R., Gavilanes, J.C., Siebe, C., Espíndola, J.M., and Rodríguez, S., 1997, The Colima Volcanic Complex: Part I: Quaternary multiple debris-avalanches deposits: Field Trip Guide, IAVCEI General Assembly, Puerto Vallarta, Mexico, January 19–24: International Association of Volcanology and Chemistry of the Earth's Interior, p. 11–14.

Lopez-Loera, H., and Gutierrez, C., 1977, Pseudosecciones geo-eléctricas e implicaciones geohidrológicas en el Valle de Colima: Geofísica Internacional, v. 17, p. 127–150.

Lopez-Loera, H., and Urrutia-Fucugauchi, J., 1996, Geophysical study of faulting associated with the Colima Volcanic Complex: Volcan de Colima Fifth International Meeting. Colima, Mexico, January 22–26, 1996, Abstract Volume: Colima, University of Colima.

Lopez-Loera, H., and Urrutia-Fucugauchi, J., 1999, Spatial and temporal magnetic anomalies of Colima volcano, western Mexico: Geofísica Internacional, v. 38, p. 3–16.

Luhr, J.F., 1981, The Colima Volcanic Complex, Mexico; Part II. Late Quaternary cinder cones: Contributions to Mineralogy and Petrology, v. 76, p. 127–147, doi: 10.1007/BF00371954.

Luhr, J.F., and Carmichael, I.S.E., 1980, The Colima Volcanic Complex, Mexico. Part I. Post-caldera andesites from Volcan Colima: Contributions to Mineralogy and Petrology, v. 71, p. 343–372, doi: 10.1007/BF00374707.

Luhr, J.F., and Carmichael, I.S.E., 1990, Geology of Volcan de Colima: Boletin Instituto Geologia, Universidad Nacional Autonoma de México, v. 107, 101 p.

Marquardt, D.W., 1963, An algorithm for least-squares estimation of non-linear parameters: Journal of the Society for Industrial and Applied Mathematics, v. 11, p. 431–441.

Nishida, Y., and Miyajima, E., 1984, Subsurface structure of Usu volcano, Japan as revealed by detail magnetic survey: Journal of Volcanology and Geothermal Research, v. 22, p. 271–281, doi: 10.1016/0377-0273(84)90005-2.

Ozima, M., and Kinoshita, H., 1964, Magnetic anisotropy of andesites in a fault zone: Journal of Geomagnetism and Geoelectricity, v. 16, p. 194–200.

Parfitt, E.A., and Peacock, D.C.P., 2001, Faulting in the south flank of Kilauea volcano, Hawaii: Journal of Volcanology and Geothermal Research, v. 106, p. 265–284, doi: 10.1016/S0377-0273(00)00247-X.

Podolsky, D.W., and Roberts, G.P., 2008, Growth of the volcano-flank Koa'e fault system, Hawaii: Journal of Structural Geology, v. 30, p. 1254–1263, doi: 10.1016/j.jsg.2008.06.006.

Rathore, J.S., and Becke, M., 1980, Magnetic fabric analyses in the Gail Valley (Carinthia, Australia) for the determination of sense of movements along this region of the Periadriatic Line: Tectonophysics, v. 69, p. 349–368, doi: 10.1016/0040-1951(80)90216-4.

Robin, C., Mossand, P., Camus, G., Cantagrel, J.M., Gourgand, A., and Vincent, P.M., 1987, Eruptive history of the Colima volcanic complex (Mexico): Journal of Volcanology and Geothermal Research, v. 31, p. 99–113, doi: 10.1016/0377-0273(87)90008-4.

Rosas-Elguera, J., and Urrutia Fucugauchi, J., 1998, The tectonic control of the volcano-sedimentary sequence of the Chapala graben, western Mexico: International Geology Review, v. 40, p. 350–362, doi: 10.1080/00206819809465214.

Rosas-Elguera, J., Ferrari, L., Garduño-Monroy, V.H., and Urrutia-Fucugauchi, J., 1996, Continental boundaries of Jalisco block and their influence in the Pliocene-Quaternary kinematics of western Mexico: Geology, v. 24, p. 921–924.

Sasai, Y., and 17 others, 1990, Volcanomagnetic effect observed during the 1986 eruption of Izu-Oshima volcano: Journal of Geomagnetism and Geoelectricity, v. 42, p. 291–317.

Stoopes, G., and Sheridan, M.F., 1992, Giant debris avalanches from the Colima volcanic complex, Mexico—Implications for long-runout landslides (>100 km) and hazard assessment: Geology, v. 20, p. 299–302, doi: 10.1130/0091-7613(1992)020<0299:GDAFTC>2.3.CO;2.

Urrutia-Fucugauchi, J., and Del Castillo, L., 1977, Un modelo del Eje Volcanico Mexicano: Boletin Sociedad Geologica Mexicana, v. 38, p. 18–28.

Urrutia-Fucugauchi, J., and Molina-Garza, R.S., 1992, Gravity modelling of regional crustal and upper mantle structure of Guerrero terrane—1, Colima graben and southern Sierra Madre Occidental, western Mexico: Geofísica Internacional, v. 31, p. 493–507.

Urrutia-Fucugauchi, J., Martin Del Pozzo, A.L., Alva-Valdivia, L.M., Lopez-Loera, H., and Ponce, R., 1997, Paleomagnetic estimates of emplacement temperatures of pyroclastic deposits from the Colima volcanic complex: IAVCEI General Assembly, January 1997, Puerto Vallarta, México. Abstract Volume: Mexico City, Mexico, International Association of Volcanology and Chemistry of the Earth's Interior.

Van Wyk de Vries, B., and Francis, P.W., 1997, Catastrophic collapses at stratovolcanoes induced by gradual volcano spreading: Nature, v. 387, p. 387–390, doi: 10.1038/387387a0.

Ventura, G., Vilardo, G., and Bruno, P.P., 1999, The role of flank failure in modifying the shallow plumbing system of volcanoes: An example from Somma-Vesuvius, Italy: Geophysical Research Letters, v. 26, p. 3681–3684, doi: 10.1029/1999GL005404.

Vezzoli, L., Tibaldi, A., Renzulli, A., Menna, M., and Flude, S., 2008, Faulting-assisted lateral collapses and influence on shallow magma feeding system at Ollague volcano (Central Volcanic Zone, Chile-Bolivia Andes): Journal of Volcanology and Geothermal Research, v. 171, p. 137–159, doi: 10.1016/j.jvolgeores.2007.11.015.

Webring, M., 1985, SAKI: A Fortran program for generalized linear inversion of gravity and magnetic profiles: U.S. Geological Survey Open-File Report 85-122, 29 p.

Manuscript Received 21 August 2008
Revised Manuscript Received 22 July 2009
Manuscript Accepted 12 September 2009